

# Dynamic Chemical Devices: Photoinduced Electron Transfer and Its Ion-Triggered Switching in Nanomechanical Butterfly-Type Bis(porphyrin)terpyridines\*\*

Myriam Linke-Schaetzel,<sup>[a, b]</sup> Christopher E. Anson,<sup>[c]</sup> Annie K. Powell,<sup>[b, c]</sup> Gernot Buth,<sup>[d]</sup> Emilio Palomares,<sup>[e, f]</sup> James D. Durrant,<sup>\*, [e]</sup> Teodor Silviu Balaban,<sup>\*, [a, b]</sup> and Jean-Marie Lehn<sup>\*, [a, b, g]</sup>

**Abstract:** A series of butterfly-type molecular constructs has been prepared in good yield by using a double Stille coupling synthetic protocol. They are composed of a terpyridine (terpy) scaffold and two wings composed of appended porphyrins that are capable of switching from an extended **W** geometry to a compact **U** geometry upon cation coordination of the terpy unit. The porphyrin moieties exist in the constructs either as free bases or they can be sequentially metallated, thus giving rise to wings of different “colours”. Stationary and time-resolved emission studies of the **HZn**, **ZnAu** and **Zn<sub>2</sub>Au** constructs show that the electronic properties are strongly dependent on the geometry. In the extended **W** conformation an energy-

transfer process is seen from the free base to the Zn-metallated porphyrin. In the **U** conformation in **Zn<sub>2</sub>Au** the donor luminescence resulting from the singlet excited state of the Zn wing is strongly, quenched not only due to the heavy atom effect but also due to a fast electron-transfer process to the ground state of the Au wing. Furthermore, the binding of ( $\alpha,\omega$ )-diamine substrates to the Zn<sup>II</sup>-porphyrin sites can also influence the conformation of the system. For the **Zn<sub>2</sub>Zn** construct, single-crystal diffraction experiments with synchro-

tron radiation allowed the structure to be solved by direct methods and fully refined; it shows the expected **U** conformation. The central Zn atom is six-coordinate, whereby the zinc atom is coordinated by the  $\eta^3$ -terpy ligand as well by monodentate and semi-chelating acetate anions. The structure is made rigid by hydrogen bonds involving the aqua ligands on the outer Zn centres and acetate oxygen atoms. The present system thus represents a double-trigger-modulated optomechanical switching device with selective substrate binding for either metal atoms or tailored ligands. Both energy- and electron-transfer processes can be controlled opening a means of improving the on/off ratio in future constructs.

**Keywords:** electron transfer • energy transfer • molecular devices • porphyrinoids • structure elucidation

[a] Dr. M. Linke-Schaetzel, Dr. habil. T. S. Balaban, Prof. J.-M. Lehn  
Forschungszentrum Karlsruhe  
Institute for Nanotechnology, Postfach 3640  
76021 Karlsruhe (Germany)  
Fax: (+49) 724-782-8298  
E-mail: silviu.balaban@int.fzk.de  
lehn@int.fzk.de

[b] Dr. M. Linke-Schaetzel, Prof. A. K. Powell, Dr. habil. T. S. Balaban,  
Prof. J.-M. Lehn  
Center for Functional Nanostructures  
University of Karlsruhe (TH), Karlsruhe (Germany)

[c] Dr. C. E. Anson, Prof. A. K. Powell  
University of Karlsruhe (TH)  
Department of Inorganic Chemistry, Karlsruhe (Germany)

[d] Dr. G. Buth  
Forschungszentrum Karlsruhe  
ANKA-Synchrotron Source and Institute for Synchrotron Radiation  
Karlsruhe (Germany)


[e] Dr. E. Palomares, Prof. J. D. Durrant  
Center for Electronic Materials and Devices  
Department of Chemistry, Imperial College London

Exhibition Road, London SW7 2 AY (UK)  
Fax: (+44) 20-7594-5801  
E-mail: jdurrant@imperial.ac.uk

[f] Dr. E. Palomares  
Institut de Ciencia Molecular (IcMol)  
Universitat de Valencia, 46100 Burjassot  
Valencia (Spain)

[g] Prof. J.-M. Lehn  
ISIS, Université Louis Pasteur  
Laboratoire de Chimie Supramoléculaire  
8, Allée Gaspard Monge, 67083 Strasbourg (France)  
Fax: (+33) 390-24-11-17  
E-mail: lehn@chimie.u-strasbg.fr

[\*\*] This is the third article in the series “Dynamic Chemical Devices” using the terpyridine scaffold. Previous papers in this series are references 19 and 20.

 Supporting information for this article is available on the WWW under <http://www.chemeurj.org/> or from the author.

**Abstract in French:** Une série d'architectures moléculaires, présentant une forme de papillon, a été préparée avec de bons rendements en utilisant une méthodologie synthétique comprenant comme étape clé un double couplage de Stille. Ces architectures sont composées d'un squelette terpyridine (terpy), qui compose le torse du papillon, sur lequel deux ailes porphyriniques ont été greffées; la géométrie peut varier entre une conformation étendue en forme de **W**, et une conformation compacte en forme de **U**, dû à la complexation du torse terpy par un cation de taille et coordination adéquate. Les ailes porphyriniques se présentent soit comme bases libres ou, peuvent être métallées successivement avec différentes métaux, pouvant ainsi avoir différentes "couleurs". Des études de fluorescence non seulement stationnaire mais aussi résolues dans le temps sur les architectures **HZn**, **ZnAu** et **Zn<sub>2</sub>Au**, montrent que les propriétés électroniques sont très dépendantes de la géométrie adoptée. Dans la conformation **W** étendue, nous avons mis en évidence un processus de transfert d'énergie de la porphyrine base libre vers la porphyrine métallée avec du Zn. Dans la conformation **U** de **Zn<sub>2</sub>Au** la luminescence de l'aile donneuse, à cause de l'état excité singulet, est fortement éteinte, non seulement à cause de l'effet d'atome lourd, mais aussi à cause d'un processus de transfert d'électron vers l'état fondamental de l'aile métallée avec de l'or. De plus, par complexation avec des ( $\alpha,\omega$ )-diamines des atomes de Zn<sup>II</sup> dans les tetrapyrroles porphyriniques, la conformation induite du système peut être profondément influencée. Pour le composé **Zn<sub>2</sub>Zn**, que nous avons pu obtenir en monocristaux, des expériences de diffraction en utilisant comme source lumineuse un synchrotron, ont fourni des données qui ont permis de résoudre la structure par des méthodes directes et de la raffiner pour montrer la conformation en **U** attendue. L'atome central de Zn a une coordination de six dont trois provenant du ligand  $\eta^3$ -terpy, et les autres de deux anions acetates, un monodenté et l'autre semi-chelatizé. La structure est ligotée par des multiples liaisons hydrogène entre des ligands aqueux sur les atomes de Zn externes et les atomes d'oxygène des anions acetates. Le système présenté est un double effecteur qui montre une commutation opto-mécanique dirigée soit par des ions métalliques, soit par d'autres ligands de taille adaptée. En même temps, les processus de transfert d'énergie et d'électrons peuvent être commutés en laissant de la place pour améliorer le rapport "on/off" dans de futures architectures.

**Abstract in Romanian:** O serie de arhitecturi moleculare având o formă de fluture au fost preparate cu randamente bune utilizând o metodologie sintetică cuprinzând ca etapă cheie un dublu cuplaj Stille. Aceste arhitecturi sunt compuse dintr-un schelet terpiridinic (terpy) alcătuiind trupul fluturelui, la care au fost implementate două aripi porfirinice care sunt capabile să varieze între o conformație extinsă în forma de literă **W** și o conformație compactă în formă de literă **U**, datorită complexării trupului terpy printr-un cation de talie și coordinație adecvată. Aripile porfirinice se prezintă fie ca baze libere sau, datorita unei metalari succesive cu diferite metale, pot avea diferite "culori". Studii de fluorescență atât staționară cât și rezolvată în timp, asupra arhitecturilor **HZn**, **ZnAu** și **Zn<sub>2</sub>Au**, arată că proprietățile electronice sunt foarte dependente de geometria adoptată. În conformația **W** extinsă, am putut pune în evidență un proces de transfer de energie dinspre baza liberă către porfirina metalată cu Zn. În conformația **U** a **Zn<sub>2</sub>Au** luminescența aripei donoare, datorate stării singulet excitate, este puternic stinsă nu numai datorită efectului de atom greu, cât și a unui proces de transfer de electron către starea fundamentală a aripei metalată cu aur. Pe deasupra, complexând ( $\alpha,\omega$ )-diamine către atomii de Zn<sup>II</sup> între tetrapirrolii porfirinici, sunt induse profunde influențe asupra conformației sistemului. Pentru compusul **Zn<sub>2</sub>Zn**, care a putut fi crescut monocristalin, experimente de difracție folosind ca sursă luminoasă un sincrotron au condus la un set de date care a permis ca structura să fie elucidată prin metode directe și rafinată, arătând conformația în **U** așteptată. Atomul central de Zn are o coordinație de șase unde pe lângă lignadul  $\eta^3$ -terpy, atomul de Zn este coordonat de către doi anioni acetat, unul monodentat, iar celălalt semi-chelatizant. Structura este brăzdată de legături de hidrogen care implică liganzii apoși situați pe centrul de Zn exteriori, și atomii de oxigen din ionii acetat. Sistemul prezentat este un dublu efector, arătând comutare opto-mecanică, datorată fie ligării prin ioni metalici, fie prin alți liganzi perfect croitorii. În același timp, atât procese de transfer de energie, cât și de electroni, pot fi perfect comutate, lăsând loc pentru îmbunătățirea raportului "on/off" în arhitecturi viitoare.

## Introduction

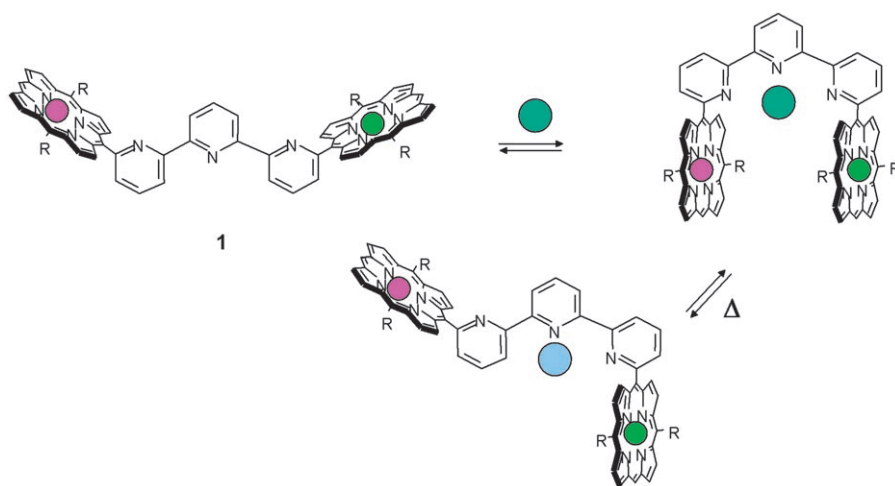
The control of molecular shape in photoactive assemblies is of interest for understanding biological processes and also for the fabrication of molecular organic photonic devices for solar-energy conversion. In nature, mechanical and electrochemical energy result from the conversion of several electrochemical and photochemical processes that are often the consequence of a change in shape at the molecular level. The dynamic structural changes of the molecular unit between different geometries can be generated either by light

excitation,<sup>[1-4]</sup> electron transfer<sup>[5,6]</sup> or ion binding.<sup>[7-11]</sup> For instance, in the photosynthetic reaction centre from *Rhodospira sphaeroides*, the secondary ubiquinone ( $Q_B$ ) moiety shows strong light-induced structural changes. In the charge-separated state  $D^+Q_AQ_B^-$  (in which D is the primary electron donor)  $Q_B^-$  is located approximately 5 Å from the  $Q_B$  position in the charge-neutral state  $DQ_AQ_B$ , having undergone a 180° propeller twist around the isoprenoid chain.<sup>[12]</sup> The consequence is that the electron-transfer rate from the primary ubiquinone  $Q_A^-$  to the secondary ubiquinone  $Q_B$  is increased by several orders of magnitude.

The design of functional architectures at the molecular level able to undergo controlled dynamic changes resulting in the modification of their properties has sparked a highly active field of research.<sup>[13–17]</sup> Recently the terpyridine scaffold was employed as a core unit for ion-triggered nanomechanical switches.<sup>[18]</sup> Thus, multistate supramolecular switching devices have been designed in which modulation of the distance between the branches of the complexes and, therefore, of the optical properties can be controlled by cation complexation or intercalation of small molecules.<sup>[19,20]</sup> The present work extends this construct to encompass porphyrins, which resemble the natural tetrapyrroles, within the reaction centre and thus control energy and electron transfer. In particular, incorporating a ligand that can change geometry as the bridge in a donor–bridge–acceptor scaffold is attractive, since the bridge can modulate the electronic coupling between the donor (D) and acceptor (A) upon host–guest interactions resulting in a change in the rate of electron transfer between D and A as observed in the natural photosynthetic system.<sup>[21,22]</sup> Examples studied so far that modulate electronic coupling between the chromophores usually use changes in redox potentials,<sup>[23–25]</sup> absorption spectra or conjugation<sup>[26,27]</sup> and, more rarely, geometric changes.<sup>[28]</sup> In the last case a large modulation of the electron-transfer event is expected, since its rate generally decreases exponentially with the distance between the donor and the acceptor.<sup>[29]</sup>

To address the role of the linker in the photophysics of porphyrin arrays, we have investigated and report herein the synthesis, characterisation and photofunction of 6,6'-bis[10,20-bis(3,5-di-*tert*-butylphenyl)porphyrin]-2,2':6',2''-terpyridine (**1**). The terpyridine (terpy) unit is normally in an extended “W” form and it adopts a closed “U” conformation upon metal-ion binding rather like a butterfly closing its wings.<sup>[19,20]</sup> Thus, it serves as a metal-gated switch to couple the porphyrins electronically. When it binds a metal ion, the pyridine groups rotate from an opened W-shape conformation to a closed or U-shape conformation, and can serve as a tweezer-type<sup>[30,31]</sup> ditopic receptor for flat substrates of appropriate size (Scheme 1).

The aim of the present work is to compare the different conformations of the constructs obtained by shape switching of the device, and the impact of the geometry on energy and/or electron transfer between the two chromophores. Recently switching behaviour upon metal-ion coordination has been described for lanthanide complexes displaying intercalative binding of DNA,<sup>[32]</sup> for  $\beta$ -sheet folding of bipyridine-



Scheme 1. Representation of the three-stage molecular-shape-switching processes induced by binding of metal ions to the terpy ligand or by heating. The different colours mean that the porphyrin moieties exist either as free bases or are coordinated to different metal atoms, which can be additionally used as triggers to switch from the W to the U conformation. Ditopic ligands such as amines can also function as triggers, while heat can induce a reversible transformation to another species.

derived peptides<sup>[33]</sup> and for tuning the electronic coupling in a bishydroquinone–terpy complex.<sup>[10]</sup>

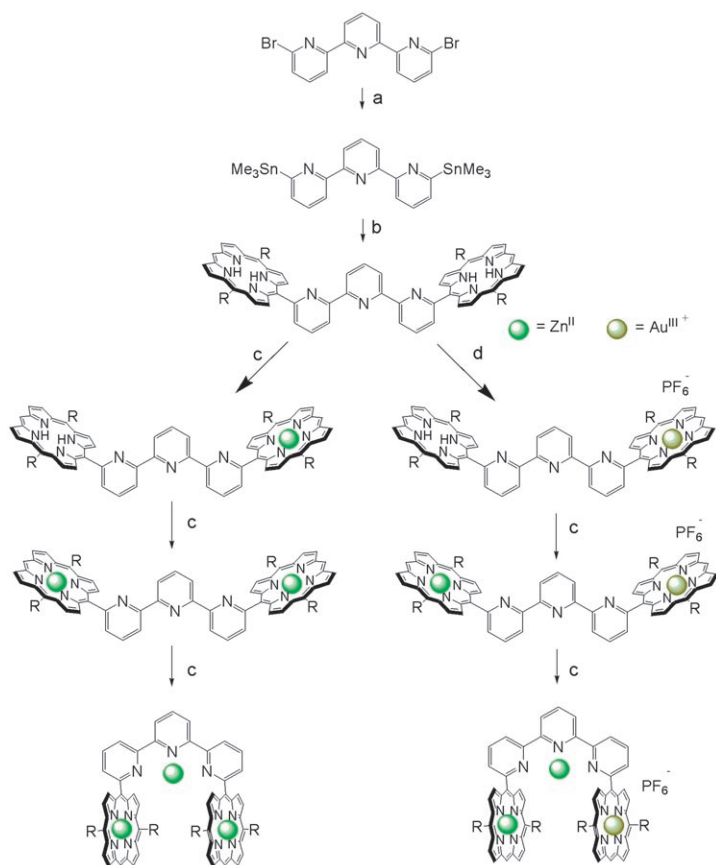
To study the electron-transfer properties in two different conformations of the constructs, both porphyrins were metallated, one with zinc(II) as an electron donor in its first excited state, and one with gold(III) as an electron acceptor in its ground state.<sup>[28]</sup> When the central terpy is not coordinated, the conformation is opened (W type), and the centre-to-centre distance between the chromophores is about 15 Å. When the terpy moiety is coordinated by a Zn<sup>II</sup> ion, the conformation closes up (U type) with a centre-to-centre distance between the porphyrins of about 7 Å.

## Results and Discussion

**Synthesis:** Compound **1** was synthesised by using a Stille coupling strategy (Scheme 2) between 6,6'-bis(trimethylstannane)-2,2':6',2''-terpyridine and 5-bromo-10,20-bis(3,5-di-*tert*-butylphenyl)porphyrin, which was readily prepared and characterised according to literature methods.<sup>[34]</sup>

This method provides relatively high quantities of the bis-porphyrinic compound, because scrambling, which is usually encountered during the classical mixed aldehyde condensation for the formation of porphyrins bearing different substituents, is absent. The two porphyrins can be individually or simultaneously metallated by Zn(OAc)<sub>2</sub>, or using the dismutation reaction of the complex [Au(tht)<sub>2</sub>]<sup>+</sup>[PF<sub>6</sub>]<sup>-</sup>, (tht = tetrahydrothiophene) a useful method developed previously to introduce Au<sup>III</sup> into non-tetraaryl porphyrins.<sup>[35]</sup> The central terpyridine can also coordinate Zn, or other divalent metals.

The conformation and thus switching ability of the ZnZn construct as a function of terpy–metal coordination, or Zn–porphyrin–amine interactions was monitored by UV-visible and NMR spectroscopy.



Scheme 2. Syntheses of the series of bisporphyrinic constructs, **ZnH<sub>2</sub>**, **ZnZn**, **Zn<sub>2</sub>Zn**, **AuH<sub>2</sub>**, **ZnAu**, **Zn<sub>2</sub>Au**. a) Sn<sub>2</sub>Me<sub>6</sub>, [Pd(PPh<sub>3</sub>)<sub>4</sub>], 90%; b) 5-bromo-10,20-bis(3,5-di-*tert*-butylphenyl)porphyrin [Pd(PPh<sub>3</sub>)<sub>4</sub>], 55%; c) Zn(OAc)<sub>2</sub>; d) [Au(tht)<sub>2</sub>]PF<sub>6</sub>, lutidine, 43%.

**Terpyridine–metal coordination:** The conformational changes resulting from coordination of the central terpy can be characterised by <sup>1</sup>H NMR spectroscopy (Figure 1). All

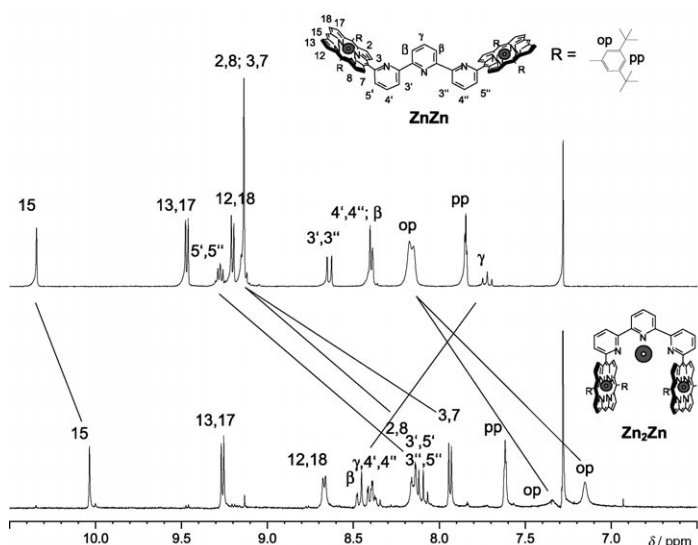


Figure 1. <sup>1</sup>H NMR spectra of the **ZnZn** and **Zn<sub>2</sub>Zn** constructs, recorded at 300 MHz in CDCl<sub>3</sub>.

the porphyrinic protons are subject to marked shielding upon complexation; in particular, the protons 2,8 and 3,7 are shifted by 1.0 and 1.2 ppm, respectively, indicating a rotation of the pyridyl groups in order to accommodate the central metal for coordination. This positions the four pyrrolic protons 2,7 and 3,8 within the ring current of the terpy moiety, thus explaining the marked high-field shifts. Furthermore, the signals of the 3,5-di-*tert*-butylphenyl protons (H<sub>op</sub> and H<sub>tBu</sub>) are split, indicative of the close proximity of the two porphyrin groups and which prevents the free rotation of the *meso*-3,5-di-*tert*-butylphenyl groups.

Absorption spectra of the reference compound 10,20-bis(3,5-di-*tert*-butylphenyl)porphyrin and of **ZnZn** show that in the latter the two porphyrin groups are quite isolated electronically. Upon terpy–metal-ion coordination, the three pyridyl rings become coplanar, and the degree of conjugation increases markedly. This results in greater electronic communication between the two porphyrinic chromophores in the ground state. As expected, when the terpy ligand is coordinated by a variety of metal ions such as Zn<sup>II</sup>, Pb<sup>II</sup>, Cu<sup>II</sup>, Mn<sup>II</sup>, the UV-spectra indicate an increase in the electronic communication between the two porphyrin groups in **ZnZn**, depending on the geometry of the central metal complex and thus on the conformation of the construct. For the **Zn<sub>2</sub>Zn** compound (Figure 2) a 4 nm blue shift and a 30% broadening of the Soret band (at FWHM) is observed, as well as a red shift in the Q-bands. For **Zn<sub>2</sub>Pb**, a 2 nm blue shift and a 9% broadening of the Soret band is observed.

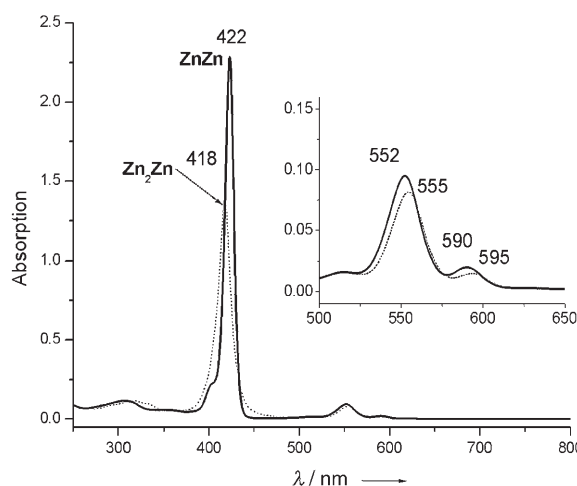


Figure 2. Absorption spectra of the **ZnZn** (full traces) and **Zn<sub>2</sub>Zn** (dotted traces) constructs, recorded in CHCl<sub>3</sub>.

**Substrate binding to the open conformation (W) of ZnZn:**

We studied the effects of addition of different (1,ω)-diamines to a solution of **ZnZn** in chloroform by NMR and UV-visible absorption spectroscopy. In the open (**W**) conformation, the distance between the two porphyrin groups as inferred from molecular models,<sup>[37]</sup> is about 15 Å, corresponding approximately to the end-to-end distances of 1,6-

hexanediamine and 1,8-octanediamine as substrates. NMR spectra of  $\text{Zn}_2\text{Zn}$ -1,8-octanediamine or  $\text{Zn}_2\text{Zn}$ -1,6-hexanediamine show a slight shift of all aromatic protons, but the spectra stay very similar to that of free  $\text{Zn}_2\text{Zn}$ . That cooperative binding is effective can be seen from the amine signals, which as a result of strong shielding are between  $-1$  and  $-5$  ppm. This shows that the substrate has been coordinated by both porphyrin groups, but the opened conformation is totally conserved so that no conformational switching has occurred. In sharp contrast, the NMR spectrum of the  $\text{Zn}_2\text{Zn}$ -DABCO (DABCO = 1,4-diazabicyclo[2.2.2]octane) adduct shows marked changes (Figure 3) similar to those

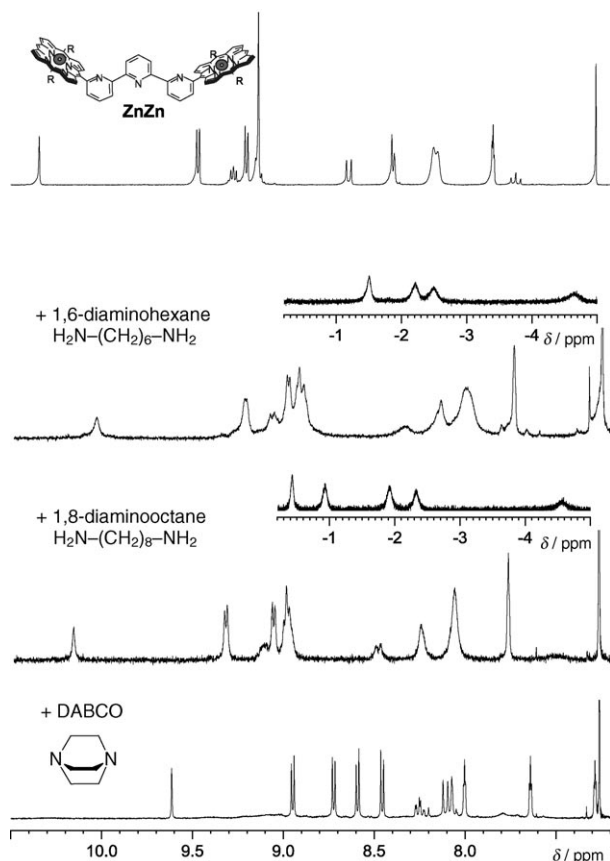


Figure 3.  $^1\text{H}$  NMR spectra recorded at 300 MHz after addition of different diamines to the construct  $\text{Zn}_2\text{Zn}$ .

produced when terpy is coordinated by zinc: all the porphyrinic protons are shielded by about 0.5 ppm, as well as the 3,3'-protons on the terpy. Again, the signal of the 3,5-phenyl protons becomes split and, due to hindered rotation, one of them being shifted. The addition of 0.7 equivalents of DABCO generates a switching in the conformation folding from an extended **W** type, open conformation to a closed **U** shape upon binding of the substrate to the  $\text{Zn}^{\text{II}}$  sites between the metallated porphyrin groups.

**Substrate binding in the closed (U) conformation of  $\text{Zn}_2\text{Zn}$ :** Figure 4 shows the  $^1\text{H}$  NMR spectra of different 1, $\omega$ -di-

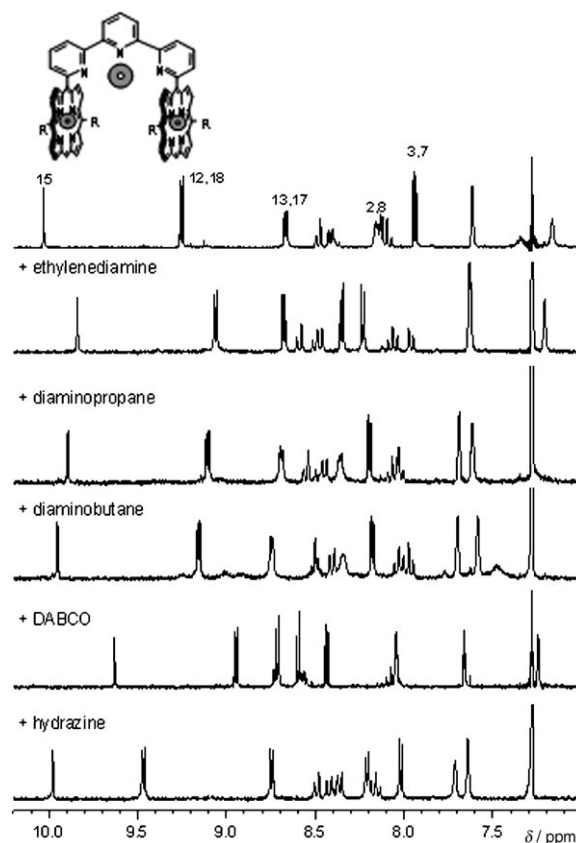


Figure 4.  $^1\text{H}$  NMR spectra recorded at 300 MHz after addition of different diamines to the  $\text{Zn}_2\text{Zn}$  construct.

amine- $\text{Zn}_2\text{Zn}$  adducts, in which the terpy unit is coordinated to zinc and the porphyrin groups approach one another. In order to produce tightly bound receptor-substrate complexes we chose short aliphatic diamines, such as 1,2-ethylenediamine, 1,4-diaminobutane, and DABCO, which was recently used in the formation of supramolecular assemblies with zinc-bisporphyrins.<sup>[36]</sup> Because of the extremely precise determination of the association constants contained within this study,<sup>[36]</sup> we have not determined the association constants for our systems in order not to duplicate research efforts, although we have previously measured the raw data (for a UV-titration example see Figure S1 in the Supporting Information). We thus refer the interested reader to this comprehensive study for the numerical values of association constants for a bisporphyrinic receptor with various diamines, including DABCO.<sup>[36]</sup> In our system, the signals of the receptor are very similar to those in absence of substrate, because the conformation is essentially fixed by the coordination of terpy to Zn and allows only small movements of the porphyrin groups. Furthermore, we were able to grow single crystals of the  $\text{Zn}_2\text{Zn}$  compound by layering a solution of  $\text{Zn}_2\text{Zn}$  in chloroform with cyclohexane (vide infra).

Upon coordination to 1,2-ethylenediamine, the pyrrolic 12,18,13,17-protons and the *meso*-porphyrin protons are slightly shielded, while the 2,8,3,7-protons are deshielded,



indicating that the two macrocycles are brought together to coordinate to both sides of the short diamine. This effect decreases as the length of the diamine increases: it is largest for 1,2-ethylenediamine and almost negligible for 1,4-butanediamine, in which the starting conformation is almost recovered. This is consistent with the distance between the two nitrogen atoms in 1,4-diaminobutane being about 6.2 Å, as inferred from molecular modelling,<sup>[37]</sup> compared to an approximately 7 Å centre-to-centre distance between the two porphyrin groups if they are considered perpendicular to the plane of the pyridine to which they are linked. Again, the amine signals are strongly shielded, resonating between 0 and -5 ppm, due to the combined ring current of the two porphyrins. When DABCO is employed as a guest, the same effects as with 1,2-ethylenediamine are observed, but these are strongly enhanced as a result of the shorter N–N distance in DABCO (about 2.8 Å) relative to the N–N distance in 1,2-ethylenediamine (about 3.7 Å). The porphyrin groups are thus clamped together in order to coordinate to both sides of the DABCO molecule.

**Coordination control by temperature:** A solution of  $Zn_2Zn$  was heated from 20 to 80 °C in toluene, and coordination evolution was monitored by NMR spectroscopy (Figure 5). During heating between 40–50 °C, a second species appears and it is present at about half of the  $Zn_2Zn$  concentration. At 80 °C, this second species is present almost exclusively. If

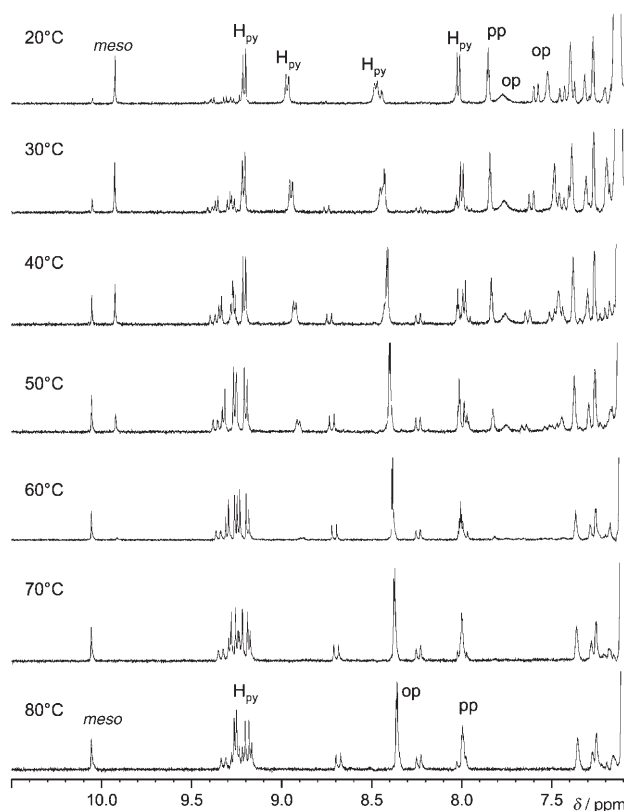


Figure 5. Variable-temperature 300 MHz  $^1H$  NMR spectra of the  $Zn_2Zn$  construct in  $[D_8]toluene$ .

the sample is cooled down, and a new spectrum is measured at 20 °C, it corresponds exactly to the initial spectrum taken at 20 °C showing that this process is completely reversible even after several cycles of heating and cooling. In the high-temperature species, all the pyrrolic protons are deshielded as well as the protons from the terpy ligand. The spectrum has several similarities with that of  $Zn_2Zn$ . Probably during the heating process the  $Zn^{II}$  ion becomes de-coordinated from one pyridine moiety, giving some degree of freedom to the other side of the construct, which can then adopt a semi-*anti* conformation (Scheme 1). Equilibration of  $Zn^{II}$  coordination between the two sides of the terpy group is probably rapid, as only one set of signals for the new compound can be seen on this NMR timescale.

From these NMR and stationary absorption spectra we conclude that this butterfly-type construct is a very versatile tool that acts as switch which can be gated by complexation, amine-coordination or heat. Its geometric features can be finely tuned by the size of the bound substrates.

**Photophysical measurements:** The  $ZnH_2$  compound in dichloromethane shows efficient energy transfer under ambient conditions from the metallated porphyrin groups to the free-base moiety, as can be seen from the steady state fluorescence emission and excitation spectra shown in Figure 6.

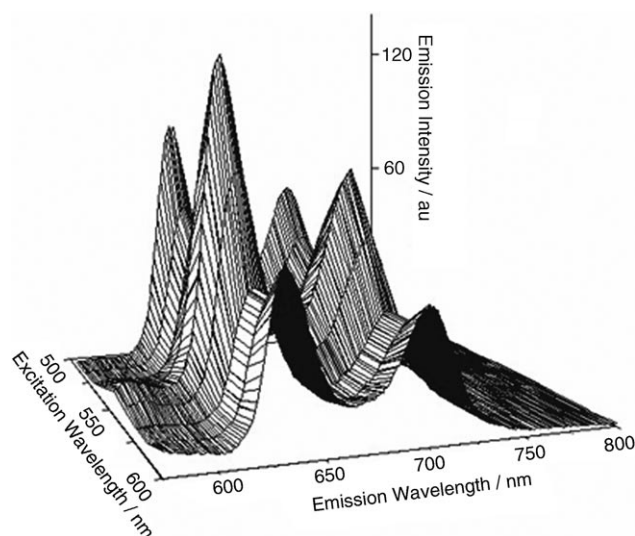


Figure 6. Three-dimensional graphical representation for the emission of the  $ZnH_2$  construct. The position of the emission bands is independent of the excitation wavelength.

The fluorescence emission spectrum of the construct reproduces the well-known emission spectra of the free-base porphyrin ( $H_2P$ ) used as a model compound, independent of the excitation wavelength, whilst the excitation spectra closely match the sum of the absorption of the  $Zn^{II}$ -*meso*-porphyrin and free-base porphyrin model compounds for this construct. Time-resolved emission studies, as shown in Figure 7, provide further support for efficient energy trans-

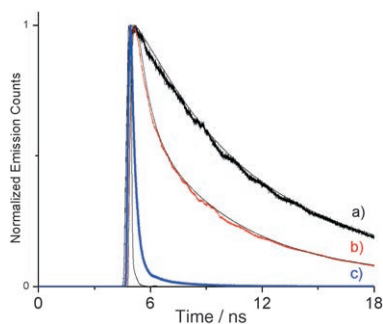


Figure 7. Emission ( $\lambda_{\text{ex}} = 404$  nm) kinetics decays for a) free-base porphyrin, b)  $\text{ZnH}_2$  and c)  $\text{ZnAu}$ . The full thin black lines represent the fit to the decays and the instrument response.

fer within the  $\text{ZnH}_2$  compound. Following 404 nm excitation, a biphasic decay is observed for the construct with lifetimes of 600 ps and 5 ns. Comparison with the model-compound emission-decay dynamics confirms the assignment of the slowest phase to singlet excited state of the free-base porphyrin of the construct. The faster 600 ps component was not observed for either model compound and is therefore assigned to energy transfer from the  $\text{Zn}^{\text{II}}$ -porphyrin to the free-base porphyrin within the construct.

We have also studied the possibility of inducing an electron transfer within the molecular construct upon light excitation. To this end, the free-base porphyrin was converted into its  $\text{Au}^{\text{III}}$  complex. Emission studies (Figure 9) of the gold porphyrin as a model for the Au-porphyrin within the construct showed only a very weak emission, which is expected as a result of the known heavy-atom effect stemming from the gold atom in the molecular structure of the porphyrin resulting in the extremely fast intersystem crossing (ISC).

Fluorescence studies for the  $\text{ZnAu}$  construct showed emission and excitation spectra characteristic of the  $\text{Zn}^{\text{II}}$ -

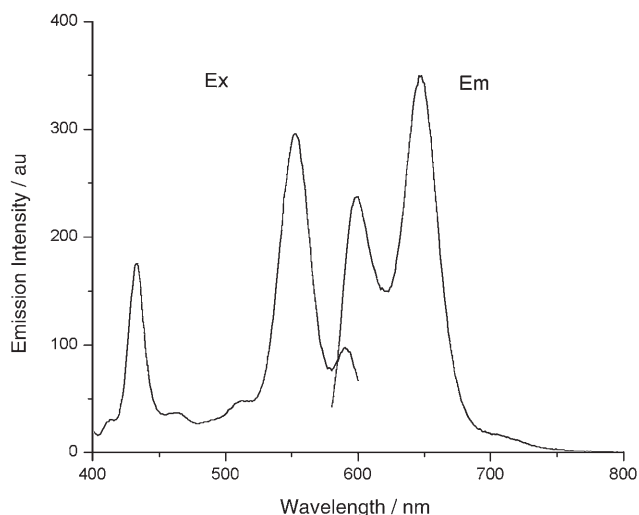


Figure 8. Emission (Em,  $\lambda_{\text{ex}} = 550$  nm) and excitation spectra (Ex,  $\lambda_{\text{em}} = 650$  nm) for the  $\text{ZnAu}$  construct in dichloromethane under ambient conditions.

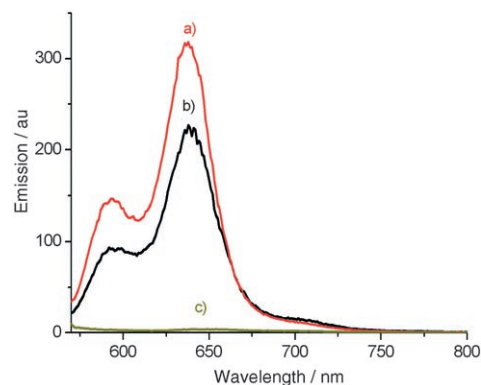


Figure 9. Emission ( $\lambda_{\text{ex}} = 550$  nm) for a) the  $\text{ZnAu}$  construct “W-shape”, b) the  $\text{Zn}_2\text{Au}$  construct “U-shape” and c) the  $\text{Au}^{\text{III}}$ -porphyrin cation. All measurements were carried out under the same conditions.

*meso*-porphyrin model compound alone (Figure 8), although the emission intensity of this construct is strongly quenched relative to the model compound. Time-resolved emission decays for the construct (Figure 7) are dominated by a fast ( $< 300$  ps) decay phase, confirming strong quenching of the emission. Following literature studies of analogous compounds,<sup>[38]</sup> this quenching is assigned to an electron-transfer process that proceeds from the  $\text{Zn}^{\text{II}}$ -porphyrin singlet excited state to the  $\text{Au}^{\text{III}}$ -porphyrin ground state of the whole construct.

The optical properties of the  $\text{ZnAu}$  construct were further studied in the presence of  $\text{Zn}^{\text{II}}$  ions. The movement from the **W** to **U** shape induced by the binding of the second  $\text{Zn}^{\text{II}}$  ions can be easily monitored by the decrease of the emission quantum yield of the construct (Figure 9). This observation can be explained by the faster quenching of the  $\text{Zn}^{\text{II}}$ -porphyrin emission by the  $\text{Au}^{\text{III}}$ -porphyrin, in good agreement with the fact that conversion to the **U** form results in a decrease in distance between the  $\text{Zn}^{\text{II}}$ -porphyrin and the  $\text{Au}^{\text{III}}$ -porphyrin within the construct. This is in line with the presence of at least two conformations, an extended **W** one, in which the  $\text{Au}^{\text{III}}$  and the  $\text{Zn}^{\text{II}}$  centres are located at a large distance from each other, and a compact, folded **U** form, in which the chromophores are in close proximity.

**Crystal Structure of the U form for  $\text{Zn}_2\text{Zn}$ :** The structure of the  $[\text{Zn}_3(\text{terpy-bisporph})(\text{O}_2\text{CCH}_3)_2(\text{OH}_2)]$  unit in  $\text{Zn}_2\text{Zn}$  is shown in Figure 10; for clarity only the *ipso*-carbon atoms of the bis(*tert*-butyl)phenyl groups are included. In the structure, both of the porphyrin rings ligate  $\text{Zn}^{2+}$  ions with Zn–N distances in the range 2.046–2.086 Å. Zn(1) and Zn(2) are additionally each coordinated by one water ligand, with Zn(1)–O(1) and Zn(2)–O(2) 2.114 and 2.120 Å, respectively. The effect of this axial coordination is to pull the Zn centres out of their respective porphyrin planes by 0.452 and 0.398 Å. The three terpy nitrogen atoms, N(9), N(10) and N(11), chelate the third Zn cation, Zn(3), such that Zn(3)–N(10) (2.096 Å) is rather shorter than the other two Zn(3)–N distances (2.344 and 2.307 Å, respectively). The coordination environment of Zn(3) is completed by oxygen atoms

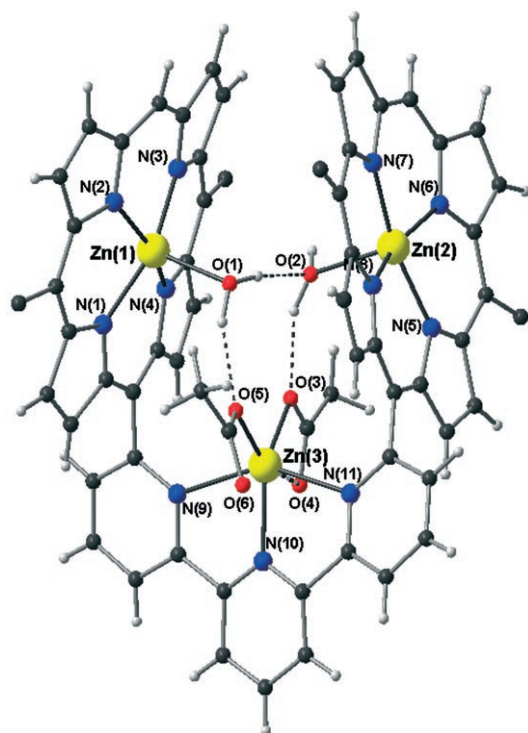


Figure 10. Crystal structure of  $\text{Zn}_2\text{Zn}$ , proving the **U** conformation. Note that the central Zn atom is chelated by the acetate anion in the back and is bound to only one oxygen atom of the front acetate anion. The two 3,5-di-*tert*-butylphenyl groups have been omitted for clarity and were replaced by the *ipso*-carbon atom. Color coding: Zn yellow, nitrogen blue, carbon black and hydrogen white spheres.

from two acetate anions. Two of these, one from each acetate, make short bonds such that  $\text{Zn}(3)\text{--O}(3)$  and  $\text{Zn}(3)\text{--O}(5)$  are 2.027 and 1.956 Å, respectively, completing a distorted trigonal-bipyramidal environment. However, the  $\text{Zn}(3)\text{--O}(4)$  distance is 2.491 Å and this acetate might best be described as semi-chelating. The  $\text{Zn}(3)\cdots\text{O}(6)$  distance, by contrast, is 2.981 Å and this ligand is therefore strictly monodentate, giving  $\text{Zn}(3)$  a six-coordinate environment.

The effect of the coordination to  $\text{Zn}(3)$  is to pull the two porphyrin rings together until they are close to parallel with the two water ligands both above the inner surfaces of their respective porphyrin moieties. Hydrogen bonding between these two ligands and from the water molecules to the acetate oxygen atoms stabilises the structure and results in pulling the porphyrins together beyond a geometry in which they are strictly parallel; the dihedral angle between the two porphyrin mean planes is 22.3°. The hydrogen bond between  $\text{O}(1)$  and  $\text{O}(2)$ , with the concomitant nonlinear  $\text{Zn}(1)\text{--O}(1)\cdots\text{O}(2)\text{--Zn}(2)$  geometry, requires that the two porphyrin systems are not eclipsed, but rather offset from each other. This reduction in molecular symmetry is reflected in the three  $\text{Zn}\cdots\text{Zn}$  separations of which  $\text{Zn}(1)\cdots\text{Zn}(3)$  at 5.365 Å is rather shorter than  $\text{Zn}(1)\cdots\text{Zn}(2)$  and  $\text{Zn}(2)\cdots\text{Zn}(3)$ , which are 5.610 and 5.630 Å, respectively. Nonetheless, the three Zn centres describe what is quite close to an equilateral triangle.

## Conclusion

We have designed a series of molecular constructs composed of a terpy scaffold and two appended porphyrin moieties capable of switching from an extended open **W** geometry to a compact closed **U** geometry upon cation coordination to the terpy unit. As a consequence, the optical properties of the constructs are reversibly modulated depending upon the geometry of the species. This represents an ion-binding-controlled reversible optomechanical switching device. Furthermore, the binding of ditopic (diamine) substrates to the  $\text{Zn}^{\text{II}}$ -porphyrin sites also depends on the conformational state of the device, thus allowing for a second substrate-selective modulation of the  $\text{W}\rightleftharpoons\text{U}$  switching process. The present system thus represents a double-trigger-modulated optomechanical switching device presenting selective substrate binding. Extensions will involve constructs with a 4,4'-biphenylene species between the terpy scaffold and two porphyrins units, thus increasing the geometrical difference between the on and off states.

## Experimental Section

**General remarks:** Solvents were dried and freshly distilled before use as follows—dichloromethane from calcium hydride; toluene and *n*-heptane from sodium metal; and  $[\text{D}]\text{chloroform}$  from phosphorous pentoxide. NMR spectra were recorded at 300 MHz ( $^1\text{H}$ ) with a Bruker DPX 300 Avance spectrometer equipped with a variable-temperature control unit. Chemical shifts are given in ppm relative to the signal of  $\text{CHCl}_3$  which was taken as  $\delta = 7.26$  (for  $^1\text{H}$ ) and 77.00 ppm (for  $^{13}\text{C}$ ). UV-visible spectra were measured with a Varian Cary 500 instrument. The variable-temperature spectra were performed by using a Peltier heating unit allowing equilibration of temperature before each curve was measured, while the solution in the quartz cuvette was stirred with a magnetic stirrer. MALDI-TOFF mass spectra were obtained on a Voyager Instrument from Applied Biosystems either with anhydrous glycerol, HABA [2'-(4-hydroxyphenylazo)benzoic acid], or 1,8,9-anthracenetriol (ditranol) matrices. HR-FAB-MS were recorded with 3-nitrobenzylalcohol (NBA) as the matrix on a Finnigan MAT 90 machine. Thin-layer chromatography was performed on silica gel plates from Macherey-Nagel. Column chromatography was performed with Merck silica gel 40–63  $\mu\text{m}$ .

**Photophysical studies:** UV-visible and fluorescence spectra were recorded in 1 cm path length quartz cell on a double beam Shimadzu spectrophotometer and Spex Fluorolog 112 Spectrofluorimeter, respectively. Transient emission data were collected by using a 404 nm excitation wavelength from an IBH NanoLED-06 pulsed laser diode (repetition rate 1 MHz, pulse duration (200 ps), intensity (~1 mW)). Emission was collected at the emission maximum for each sample using a Hamamatsu microchannel plate with an instrument response of 350 ps. Data were collected for matched data collection times of 2500 s.

**X-ray crystallography:** Data were measured on a Stoe IPDS II area detector diffractometer on the ANKA-SCD beamline at the ANKA synchrotron source at the Forschungszentrum Karlsruhe, by using Si-monochromated radiation of wavelength 0.79999 Å. The crystal was cooled to 150 K, and a hemisphere of data was measured to a resolution of 0.88 Å. Crystals of  $\text{Zn}_2\text{Zn}$  grown from  $\text{CHCl}_3/\text{cyclohexane}$  mixtures formed very thin red needles that were very weakly diffracting, particularly at higher angles even using synchrotron radiation and this was reflected both in the high value for  $R_{\text{int}}$  and the values for  $wR_2$  and  $R_1$ . However, the data are more than adequate to demonstrate the overall conformation of the molecule. Details of the ANKA-SCD beamline are given in reference [39].



The structure was solved by direct methods and refined by blocked full-matrix refinement against  $F^2$  (all data) using SHELXTL.<sup>[40]</sup> Most of the structure was fully ordered, but one cyclohexane molecule (atoms C-(401)–C(414)) was badly disordered and no attempt was made to allocate the partial atoms into overlapping molecules. A further solvent molecule could be refined as superimposed chloroform and cyclohexane molecules, each of half occupancy, by using a combination of geometrical restraints and similarity restraints for the thermal parameters.

Crystal data for **Zn<sub>2</sub>Zn-2.5 CHCl<sub>3</sub>·2.5 C<sub>6</sub>H<sub>12</sub>·H<sub>2</sub>O**: C<sub>132.5</sub>H<sub>159.5</sub>Cl<sub>7.5</sub>N<sub>11</sub>Zn<sub>3</sub>,  $M_r = 2480.20$  g mol<sup>-1</sup>, monoclinic, space group  $P2_1/c$ ,  $a = 21.2921(10)$ ,  $b = 15.4541(8)$ ,  $c = 39.8009(15)$  Å,  $\beta = 99.035(3)^\circ$ ,  $V = 12934.0(10)$  Å<sup>3</sup>,  $Z = 4$ ,  $T = 150(2)$  K,  $F(000) = 5220$ ,  $\rho_{\text{calcd}} = 1.274$  Mg m<sup>-3</sup>,  $\mu(0.79999 \text{ \AA}) = 0.867$  mm<sup>-1</sup>, red needle  $0.42 \times 0.02 \times 0.02$  mm, 52587 data measured, of which 17222 unique ( $R_{\text{int}} = 0.3039$ ) and 8889 observed with  $I > 2\sigma(I)$ ,  $2\theta_{\text{max}} = 51.5^\circ$ ; 1473 parameters and 26 restraints,  $wR_2 = 0.3351$ ,  $S = 1.051$  (all data),  $R_1 = 0.1265$  [ $> 2\sigma(I)$ ], final difference max peak/hole =  $+0.78/-1.26$  e Å<sup>-3</sup>.

CCDC 275116 contains the supplementary crystallographic data for this paper. These data can be obtained free of charge from The Cambridge Crystallographic Data Centre via [www.ccdc.cam.ac.uk/data\\_request/cif](http://www.ccdc.cam.ac.uk/data_request/cif).

**6,6''-Bis(trimethylstannane)-2,2':6,2''-terpyridine (1)**: A solution of 6,6''-dibromo-2,2':6,2''-terpyridine (200 mg, 0.51 mmol), hexamethyldistannane (468 mg, 1.43 mmol) and tetrakis(triphenylphosphine)palladium (50 mg, 0.043 mmol) in toluene (10 mL) was heated to reflux during 20 h. The crude mixture was then filtered on a Celite pad and the solvent evaporated. Recrystallisation from CH<sub>2</sub>Cl<sub>2</sub>/hexane, filtration of the solid (impure product) and evaporation of the remaining solution gave pure **1** (250 mg, 90%). <sup>1</sup>H NMR (300 MHz, CDCl<sub>3</sub>):  $\delta = 8.56$  (d,  $^3J = 7.8$  Hz, 2H; H<sub>5,5'</sub>), 8.50 (dd,  $^3J = 8.1$  Hz,  $^5J = 1.2$  Hz, 2H; H<sub>3,3'</sub>), 7.94 (t,  $^3J = 7.8$  Hz, 1H; H<sub>4</sub>), 7.68 (t,  $^3J = 8.1$  Hz, 2H; H<sub>4,4'</sub>), 7.46 (dd,  $^3J = 7.5$  Hz,  $^5J = 1.5$  Hz, 2H; H<sub>3,5'</sub>), 0.39 ppm (s, 18H; Me); Maldi-TOFF-MS:  $m/z$  calcd for C<sub>21</sub>H<sub>27</sub>N<sub>3</sub>Sn<sub>2</sub>: 558.85; found: 559.93.

**6,6''-Bis[10,20-bis(3,5-di-*tert*-butylphenyl)porphyrin]-2,2':6,2''-terpyridine (H<sub>2</sub>H<sub>2</sub>)**: A solution of **1** (65 mg, 0.118 mmol), 5-bromo-10,20-bis(3,5-di-*tert*-butylphenyl)porphyrin (150 mg, 0.196 mmol) and tetrakis(triphenylphosphine)palladium (11.3 mg, 0.0097 mmol) in toluene (20 mL) was heated to reflux during 84 h. After addition of water and extraction with CH<sub>2</sub>Cl<sub>2</sub>, the crude mixture was purified by column chromatography on SiO<sub>2</sub> (eluent: CH<sub>2</sub>Cl<sub>2</sub>/hexane 30:70) to leave pure **H<sub>2</sub>H<sub>2</sub>** (90 mg, 55%) as a violet solid. <sup>1</sup>H NMR (300 MHz, CDCl<sub>3</sub>):  $\delta = 10.28$  (s, 2H; H<sub>15</sub>), 9.38 (d,  $^3J = 4.5$  Hz, 4H; H<sub>13,17</sub>), 9.29 (d,  $^3J = 7.2$  Hz,  $^4J = 1.8$  Hz, 2H; H<sub>5,5'</sub>), 9.11 (d,  $^3J = 4.5$  Hz, 4H; H<sub>12,18</sub>), 9.03 (s, 8H; H<sub>2,8,3,7</sub>), 8.67 (d,  $^3J = 7.8$  Hz, 2H; H<sub>3,3'</sub>), 8.40 (t,  $^3J = 7.5$  Hz, 2H; H<sub>4,4'</sub>), 8.35 (m, 2H; H<sub>6</sub>), 8.14 (brs br, 8H; H<sub>op</sub>), 7.84 (t,  $^4J = 1.8$  Hz, 4H; H<sub>pp</sub>), 7.75 (t,  $^3J = 7.8$  Hz, 1H; H<sub>7</sub>), 1.58 (s, 72H; H<sub>tBu</sub>), -3.11 ppm (s, 4H; NH); UV/Vis (CHCl<sub>3</sub>):  $\lambda_{\text{max}} = 418, 411, 547, 579, 638$  nm; Maldi-TOFF-MS:  $m/z$  calcd for C<sub>111</sub>H<sub>115</sub>N<sub>11</sub>: 1603.21; found: 1602.43.

**6-[10-(3,5-Di-*tert*-butylphenyl)porphyrin]-6''-[20-(3,5-di-*tert*-butylphenyl)porphyrinatozinc]-2,2':6,2''-terpyridine (ZnH<sub>2</sub>)**: A solution of **H<sub>2</sub>H<sub>2</sub>** (20 mg, 0.0125 mmol), and zinc acetate (2.7 mg, 0.015 mmol) was stirred at room temperature in a mixture of CHCl<sub>3</sub> (10 mL) and MeOH (3 mL) for 2 h. After evaporation of the solvent, the residue was taken up in CH<sub>2</sub>Cl<sub>2</sub>, was washed with water and was evaporated. The crude mixture was purified by column chromatography on SiO<sub>2</sub> (eluent: CH<sub>2</sub>Cl<sub>2</sub>/hexane 50:50) to leave pure **ZnH<sub>2</sub>** (6 mg, 30%) as a pink solid. <sup>1</sup>H NMR (300 MHz, CDCl<sub>3</sub>):  $\delta = 10.39$  (s, 1H; H<sub>15Zn</sub>), 10.32 (s, 1H; H<sub>15H<sub>2</sub></sub>), 9.50 (d,  $^3J = 4.5$  Hz, 2H; H<sub>13,17</sub>), 9.43 (d,  $^3J = 4.5$  Hz, 2H; H<sub>13,17</sub>), 9.33 (m, 2H; H<sub>5,5'</sub>), 9.24 (d,  $^3J = 4.5$  Hz, 2H; H<sub>12,18</sub>), 9.17 (s, 4H; H<sub>por2,8,7,3</sub>), 9.14 (d,  $^3J = 4.8$  Hz, 2H; H<sub>12,18</sub>), 9.07 (s, 4H; H<sub>por2,8,3,7</sub>), 8.71 (d,  $^3J = 7.8$  Hz, 2H; H<sub>3,3'</sub>), 8.43 (m, 4H; H<sub>4,4',\beta</sub>), 8.18 (brs, 8H; H<sub>op</sub>), 7.87 (brs, 4H; H<sub>pp</sub>), 7.75 (t,  $^3J = 8.1$  Hz, 1H; H<sub>7</sub>), 1.60 (s, 36H; H<sub>tBu</sub>), 1.59 (s, 36H; H<sub>tBu</sub>), -2.82 ppm (s, 2H; NH); UV/Vis (CHCl<sub>3</sub>):  $\lambda_{\text{max}} = 418, 411, 547, 579, 638$  nm; Maldi-TOFF-MS:  $m/z$  calcd for C<sub>111</sub>H<sub>113</sub>N<sub>11</sub>Zn: 1666.57; found: 1665.56.

**6,6''-Bis[10,20-bis(3,5-di-*tert*-butylphenyl)porphyrinatozinc]-2,2':6,2''-terpyridine (ZnZn)**: A solution of **ZnH<sub>2</sub>** (20 mg, 0.0125 mmol), and zinc acetate (5 mg, 0.027 mmol) was stirred at room temperature in a mixture of CHCl<sub>3</sub> (10 mL) and MeOH (3 mL) for 2 h. After evaporation of the sol-

vent, the residue was taken up in CH<sub>2</sub>Cl<sub>2</sub>, was washed with water and was evaporated. The crude mixture was purified by column chromatography on SiO<sub>2</sub> (eluent: CH<sub>2</sub>Cl<sub>2</sub>/hexane 50:50) to leave pure **ZnZn** (16 mg, 75%) as a pink solid. <sup>1</sup>H NMR (300 MHz, CDCl<sub>3</sub>):  $\delta = 10.34$  (s, 2H; H<sub>15</sub>), 9.47 (d,  $^3J = 4.5$  Hz, 4H; H<sub>13,17</sub>), 9.28 (m, 2H; H<sub>5,5'</sub>), 9.21 (d,  $^3J = 4.5$  Hz, 4H; H<sub>12,18</sub>), 9.13 (s, 8H; H<sub>2,8,7,3</sub>), 8.64 (d,  $^3J = 7.8$  Hz, 2H; H<sub>3,3'</sub>), 8.39 (m, 4H; H<sub>4,4',\beta</sub>), 8.16 (brs, 8H; H<sub>op</sub>), 7.84 (brs, 4H; H<sub>pp</sub>), 7.72 (t,  $^3J = 7.8$  Hz, 1H; H<sub>7</sub>), 1.58 ppm (s, 72H; H<sub>tBu</sub>); UV/Vis (CHCl<sub>3</sub>):  $\lambda_{\text{max}} = 422, 552, 590$  nm; Maldi-TOFF-MS:  $m/z$  calcd for C<sub>111</sub>H<sub>111</sub>N<sub>11</sub>Zn<sub>2</sub>: 1729.94; found: 1729.75.

**6-[10-(3,5-Di-*tert*-butylphenyl)porphyrin]-6''-[20-(3,5-di-*tert*-butylphenyl)porphyrinatozinc]-2,2':6,2''-terpyridinezinc (Zn<sub>2</sub>Zn)**:

a) A solution of **ZnH<sub>2</sub>** (5 mg, 0.0031 mmol), and zinc acetate (1.7 mg, 0.009 mmol) was stirred at room temperature in a mixture of CHCl<sub>3</sub> (4 mL) and MeOH (1 mL) for 1 h. After evaporation of the solvent, the residue was taken up in CH<sub>2</sub>Cl<sub>2</sub> and washed with water and evaporated to leave pure **Zn<sub>2</sub>Zn** (5.5 mg, 100%) as a pink solid.

b) A solution of 6,6''-bis-(10,20-bis(3,5-di-*tert*-butylphenyl)porphyrinatozinc)-2,2':6,2''-terpyridine (**ZnZn**) (5 mg, 0.0029 mmol), and zinc acetate (0.5 mg, 0.0029 mmol) was stirred at room temperature in a mixture of CHCl<sub>3</sub> (4 mL) and MeOH (1 mL) for 15 min. After evaporation of the solvent, the residue was taken up in CH<sub>2</sub>Cl<sub>2</sub> and washed with water and evaporated to leave pure **Zn<sub>2</sub>Zn** (5.5 mg, 100%) as a pink solid. <sup>1</sup>H NMR (300 MHz, CDCl<sub>3</sub>):  $\delta = 10.00$  (s, 2H; H<sub>15</sub>), 9.22 (d,  $^3J = 4.5$  Hz, 4H; H<sub>13,17</sub>), 8.65 (d,  $^3J = 4.5$  Hz, 2H; H<sub>12,18</sub>), 8.46 (d,  $^3J = 7.2$  Hz, 2H; H<sub>6</sub>), 8.39 (m, 2H; H<sub>3,3'</sub>), 8.15 (d,  $^3J = 4.5$  Hz, 4H; H<sub>8,2</sub>), 8.08 (m, 5H; H<sub>7,4',4'',5,5'</sub>), 7.95 (d,  $^3J = 4.5$  Hz, 4H; H<sub>7,3</sub>), 7.64 (brs, 4H; H<sub>pp</sub>), 7.38 (brs, 4H; H<sub>op</sub>), 7.17 (brs, 4H; H<sub>op</sub>), 1.37 ppm (s, 72H; H<sub>tBu</sub>); UV/Vis (CHCl<sub>3</sub>):  $\lambda_{\text{max}} = 418, 555, 595$  nm; Maldi-TOFF-MS (anthracenetriol used as matrix):  $m/z$  calcd for C<sub>111</sub>H<sub>111</sub>N<sub>11</sub>Zn<sub>3</sub>: 1795.3; found: 2018.75 [ $M^+$ +anthracenetriol].

**6-[10-(3,5-Di-*tert*-butylphenyl)porphyrin]-6''-[20-(3,5-di-*tert*-butylphenyl)porphyrinatogold]-2,2':6,2''-terpyridine hexafluorophosphate (H<sub>2</sub>Au)**:

Compound **H<sub>2</sub>H<sub>2</sub>** (35 mg, 0.022 mmol) and complex [Au(tht)<sub>2</sub>PF<sub>6</sub>]<sup>[6]</sup> (35 mg, 0.068 mmol) were placed in a flask under argon. CHCl<sub>3</sub> (20 mL) and a solution of lutidine in CHCl<sub>3</sub> (0.07 M, 0.6 mL) were then added to the flask. The reaction mixture was refluxed for 3 h and subsequently evaporated. The crude mixture was purified by column chromatography on Al<sub>2</sub>O<sub>3</sub> (eluent: CH<sub>2</sub>Cl<sub>2</sub>) to leave pure **H<sub>2</sub>Au** (14 mg, 34%) as a red solid. Unreacted starting material could also be cleanly recovered (15 mg, 43%). <sup>1</sup>H NMR (300 MHz, CDCl<sub>3</sub>):  $\delta = 11.33$  (s, 1H; H<sub>15Au</sub>), 10.29 (s, 1H; H<sub>15H<sub>2</sub></sub>), 9.98 (d,  $^3J = 4.8$  Hz, 2H; H<sub>13,17</sub>), 9.51 (d,  $^3J = 5.1$  Hz, 2H; H<sub>12,18</sub>), 9.50 (m, 4H; H<sub>por8,2,7,3</sub>), 9.42 (m, 1H; H<sub>6</sub>), 9.39 (d,  $^3J = 4.8$  Hz, 2H; H<sub>13,17</sub>), 9.10 (d,  $^3J = 4.5$  Hz, 2H; H<sub>12,18</sub>), 9.04 (d,  $^3J = 4.8$  Hz, 2H; H<sub>por7,3</sub>), 9.01 (d,  $^3J = 4.8$  Hz, 2H; H<sub>por8,2</sub>), 8.70 (d,  $^3J = 8.1$  Hz, 1H; H<sub>2</sub>), 8.56 (m, 2H; H<sub>7,5</sub>), 8.41 (m, 3H; H<sub>6,3',4'</sub>), 8.14 (brs, 8H; H<sub>op</sub>), 7.98 (t, 2H; H<sub>pp</sub>,  $^4J = 1.8$  Hz), 7.84 (t,  $^4J = 1.8$  Hz, 2H; H<sub>pp</sub>), 7.78 (t,  $^3J = 8.1$  Hz, 1H; H<sub>7</sub>), 1.58 (s, 36H; H<sub>tBu</sub>), 1.57 (s, 36H; H<sub>tBu</sub>), -2.89 ppm (s, 2H; NH); UV/Vis (CHCl<sub>3</sub>):  $\lambda_{\text{max}} = 414, 513, 542, 583, 638$  nm; Maldi-TOFF-MS:  $m/z$  calcd for C<sub>111</sub>H<sub>113</sub>N<sub>11</sub>Au: 1798.16; found: 1798.25.

**6-[10-(3,5-Di-*tert*-butylphenyl)porphyrinatozinc]-6''-[20-(3,5-di-*tert*-butylphenyl)porphyrinatogold]-2,2':6,2''-terpyridine hexafluorophosphate (ZnAu)**:

A solution of **H<sub>2</sub>Au** (10 mg, 0.0051 mmol), and zinc acetate (9.5 mg, 0.051 mmol) was stirred at room temperature in a mixture of CHCl<sub>3</sub> (5 mL) and MeOH (1 mL) for 30 min. After evaporation of the solvent, the residue was taken up in CH<sub>2</sub>Cl<sub>2</sub>, was washed with water and was evaporated. The crude mixture was purified by column chromatography on Al<sub>2</sub>O<sub>3</sub> (eluent: CH<sub>2</sub>Cl<sub>2</sub>) to leave pure **ZnAu** (8.3 mg, 80%) as a red solid. <sup>1</sup>H NMR (300 MHz, CDCl<sub>3</sub>):  $\delta = 11.31$  (s, 1H; H<sub>15Au</sub>), 10.32 (s, 1H; H<sub>15Zn</sub>), 9.95 (d,  $^3J = 5.1$  Hz, 2H; H<sub>13,17</sub>), 9.47 (m, 8H; H<sub>por12,18,8,2,7,3,13,17</sub>), 9.38 (d,  $^3J = 8.1$  Hz, 1H; H<sub>6</sub>), 9.22 (m, 1H; H<sub>5</sub>), 9.18 (d,  $^3J = 4.5$  Hz, 2H; H<sub>12,18</sub>), 9.12 (d,  $^3J = 4.8$  Hz, 2H; H<sub>por7,3</sub>), 9.10 (d,  $^3J = 4.5$  Hz, 2H; H<sub>por8,2</sub>), 8.67 (d,  $^3J = 8.1$  Hz, 1H; H<sub>2</sub>), 8.54 (t,  $^3J = 8.1$  Hz, 1H; H<sub>7</sub>), 8.48 (d,  $^3J = 8.1$  Hz, 1H; H<sub>5</sub>), 8.39 (m, 3H; H<sub>6,4',3'</sub>), 8.14 (s, 4H; H<sub>op</sub>), 8.11 (s, 4H; H<sub>op</sub>), 7.95 (s, 2H; H<sub>pp</sub>), 7.82 (s, 2H; H<sub>pp</sub>), 7.72 (t,  $^3J = 8.1$  Hz, 1H; H<sub>4</sub>), 1.59 (s, 36H; H<sub>tBu</sub>), 1.58 ppm (s, 36H; H<sub>tBu</sub>); UV/Vis (CHCl<sub>3</sub>):  $\lambda_{\text{max}} = 406, 424$  (sh), 517, 554 nm; Maldi-TOFF-MS:  $m/z$  calcd for C<sub>111</sub>H<sub>111</sub>N<sub>11</sub>AuZn: 1861.52; found: 1859.35.

**6-[10-(3,5-Di-*tert*-butylphenyl)porphyrinatozinc]-6''-(20-(3,5-di-*tert*-butylphenyl)porphyrinatogold(III)-2,2':6',2''-terpyridinezinc hexafluorophosphate (Zn<sub>2</sub>Au)**: A solution of ZnAu (10 mg, 0.0051 mmol), and zinc acetate (0.9 mg, 0.0051 mmol) was stirred at room temperature in a mixture of CHCl<sub>3</sub> (5 mL) and MeOH (1 mL) for 30 min. Evaporation of the solvent gave pure Zn<sub>2</sub>Au (8.3 mg, 80%) as a red solid. <sup>1</sup>H NMR (300 MHz, CDCl<sub>3</sub>): δ = 10.84 (s, 1H; H<sub>15Au</sub>), 9.32 (s, 1H; H<sub>15Zn</sub>), 9.80 (d, <sup>3</sup>J = 4.8 Hz, 2H; H<sub>13,17</sub>), 9.30 (d, <sup>3</sup>J = 4.2 Hz, 2H; H<sub>13,17</sub>), 9.13 (d, <sup>3</sup>J = 4.8 Hz, 2H; H<sub>12,18</sub>), 8.72 (d, <sup>3</sup>J = 4.5 Hz, 2H; H<sub>12,18</sub>), 8.63 (m, 4H; H<sub>por8,2</sub>, H<sub>por3,5</sub>), 8.59 (d, <sup>3</sup>J = 7.8 Hz, 1H; H<sub>β</sub>), 8.50 (m, 2H; H<sub>γ,5</sub>), 8.39 (d, <sup>3</sup>J = 4.8 Hz, 2H; H<sub>por7,3</sub>), 8.37 (m, 1H; H<sub>α'</sub>), 8.23 (m, 3H; H<sub>por8,2</sub>, H<sub>β,4</sub>), 8.10 (d, <sup>3</sup>J = 7.8 Hz, 1H; H<sub>3</sub>), 8.00 (d, <sup>3</sup>J = 4.5 Hz, 2H; H<sub>por7,3</sub>), 7.78 (brs, 2H; H<sub>ppZn</sub>), 7.61 (brs, 2H; H<sub>ppAu</sub>), 7.53 (s, 2H; H<sub>opZn</sub>), 7.42 (s, 2H; H<sub>opAu</sub>), 7.22 (s, 2H; H<sub>opAu</sub>), 7.16 (s, 2H; H<sub>opZn</sub>), 1.37 ppm (s, 72H; H<sub>tBu</sub>); UV/Vis (CHCl<sub>3</sub>): λ<sub>max</sub> = 410 (sh), 422, 517, 554 nm; Maldi-TOFF-MS: *m/z* calcd for C<sub>111</sub>H<sub>111</sub>N<sub>11</sub>Au<sub>2</sub>Zn<sub>2</sub>: 1926.90; found: 1860.48 (central Zn not seen).

## Acknowledgements

E.P. acknowledges the award of a Marie Curie Research Fellowship. The research work in Karlsruhe and ML-S were partially supported by the Deutsche Forschungsgemeinschaft (DFG) through the Center for Functional Nanostructures (CFN) of the University of Karlsruhe through former projects C3.2 and C3.6 and current project C3.5.

- [1] V. Balzani, A. Credi, F. M. Raymo, J. F. Stoddart, *Angew. Chem.* **2000**, *112*, 3484–3530; *Angew. Chem. Int. Ed.* **2000**, *39*, 3348–3339.
- [2] *Molecular Switches* (Ed.: B. Feringa), Wiley-VCH, Weinheim, **2001**, pp. 124–138.
- [3] B. Wegewijs, R. M. Hermant, J. W. Verhoeven, A. G. M. Kunst, R. P. H. Rettschnick, *Chem. Phys. Lett.* **1987**, *140*, 587–590.
- [4] X. Y. Lauteslager, M. J. Bartels, J. J. Pier, J. M. Warman, J. W. Verhoeven, A. M. Brouwer, *Eur. J. Org. Chem.* **1998**, 2467–2481.
- [5] S. Shinkai, T. Nakaji, T. Ogawa, K. Shigematsu, O. Manabe, *J. Am. Chem. Soc.* **1981**, *103*, 111–115.
- [6] V. Pallavicini, M. Pedrazzini, M. Zema, *Chem. Eur. J.* **1999**, *5*, 3679–3688.
- [7] M. J. Chmielewski, A. Szumna, J. Jurczak, *Tetrahedron Lett.* **2004**, *45*, 8699–8703.
- [8] M. Barboiu, G. Vaughan, N. Kyritsakas, J.-M. Lehn, *Chem. Eur. J.* **2003**, *9*, 763–769.
- [9] A.-M. Stadler, N. Kyritsakas, J.-M. Lehn, *Chem. Commun.* **2004**, 2024–2025.
- [10] M. Büschel, M. Helldobler, J. Daub, *Chem. Commun.* **2003**, 1338–1339.
- [11] J. F. Stoddart, *Acc. Chem. Res.* **2001**, *34*, 409–522.
- [12] M. H. B. Stowell, T. M. McPhillips, D. C. Rees, S. M. Soltis, E. Abresch, G. Feher, *Science* **1997**, *276*, 812–816.
- [13] “Photochemical and Photophysical Devices”: V. Balzani, F. Scandola, in *Comprehensive Supramolecular Chemistry* (Ed.: D. N. Reinhoudt), Oxford, Pergamon, **1996**, pp. 688–746.
- [14] M. Harmjan, H. S. Gill, M. J. Scott, *J. Am. Chem. Soc.* **2000**, *122*, 10476–10477.
- [15] G. McSkimming, J. H. R. Tucker, H. Bouas-Laurent, J.-P. Desvergne, *Angew. Chem.* **2000**, *112*, 2251–2253; *Angew. Chem. Int. Ed.* **2000**, *39*, 2167–2169.
- [16] T. Szabo, G. Hilmersson, J. Rebek, *J. Am. Chem. Soc.* **1998**, *120*, 6193–6194.
- [17] E. I. Zenkevich, A. M. Shulga, U. Rempel, J. von Richthofen, C. von Borczyskowski, *J. Lumin.* **1998**, *76/77*, 354–358.
- [18] J.-P. Collin, P. Gavina, J.-P. Sauvage, *Chem. Commun.* **1996**, 2005–2006.
- [19] M. Barboiu, L. Prodi, M. Montalti, N. Zaccheroni, N. Kyritsakas, J.-M. Lehn, *Chem. Eur. J.* **2004**, *10*, 2953–2959.
- [20] A. Petitjean, R. G. Khoury, N. Kyritsakas, J.-M. Lehn, *J. Am. Chem. Soc.* **2004**, *126*, 6637–6647.
- [21] “Covalently Linked Systems Based on Organic Components”: M. N. Paddon-Row, in *Electron Transfer in Chemistry* (Ed.: V. Balzani), Wiley-VCH, Weinheim, **2003**, pp. 179–271.
- [22] “Electron and Energy Transfer”: M. N. Paddon-Row in *Stimulating Concepts in Chemistry* (Eds.: F. Vögtle, J. F. Stoddart, M. Shibasaki), Wiley-VCH, Weinheim, **2000**, pp. 267–291.
- [23] S. Higashida, H. Tsue, K. Sugiura, T. Kaneda, Y. Sakata, Y. Tanaka, S. Taniguchi, T. Okada, *Bull. Chem. Soc. Jpn.* **1996**, *69*, 1329–1335.
- [24] C. Clausen, D. T. Gryko, A. A. Yasser, J. R. Diers, D. F. Bocian, W. G. Kuhr, J. S. Lindsey, *J. Org. Chem.* **2000**, *65*, 7371–7378.
- [25] M. Andersson, M. Linke, J.-C. Chambron, J. Davidsson, V. Heitz, L. Hammarström, J.-P. Sauvage, *J. Am. Chem. Soc.* **2002**, *124*, 4347–4367.
- [26] K. Sendt, L. A. Johnston, W. A. Hough, M. J. Crossley, N. S. Hush, J. R. Reimers, *J. Am. Chem. Soc.* **2002**, *124*, 9299–9309.
- [27] F. Blomgren, S. Larsson, S. F. Nelsen, *J. Comput. Chem.* **2001**, *22*, 655–664.
- [28] M. Linke, J.-C. Chambron, V. Heitz, J.-P. Sauvage, S. Encinas, F. Barigelletti, L. Flamigni, *J. Am. Chem. Soc.* **2000**, *122*, 11834–11844.
- [29] R. A. Marcus, N. Sutin, *Biochim. Biophys. Acta* **1985**, *811*, 265–322.
- [30] F. G. Klärner, J. Panitzky, D. Blaser, R. Boese, *Tetrahedron* **2001**, *57*, 3673–3687.
- [31] S. C. Zimmerman, C. M. VanZyl, G. S. Hamilton, *J. Am. Chem. Soc.* **1989**, *111*, 1373–1381.
- [32] P. B. Glover, P. R. Ashton, L. J. Childs, A. Rodger, M. Kercher, R. M. Williams, L. De Cola, Z. Pikramenou, *J. Am. Chem. Soc.* **2003**, *125*, 9918–9919.
- [33] J. P. Schneider, J. W. Kelly, *J. Am. Chem. Soc.* **1995**, *117*, 2533–2546.
- [34] T. S. Balaban, R. Goddard, M. Linke-Schaetzel, J.-M. Lehn, *J. Am. Chem. Soc.* **2003**, *125*, 4233–4239.
- [35] J.-C. Chambron, V. Heitz, J.-P. Sauvage, *New J. Chem.* **1997**, *21*, 237–240.
- [36] P. Ballester, A. Costa, A. M. Castilla, P. M. Deyà, A. Frontera, R. M. Gomila, C. A. Hunter, *Chem. Eur. J.* **2005**, *11*, 2196–2206.
- [37] HyperChem®, Release 7, HyperCube Inc, Gainesville, Florida 32601, **2002**.
- [38] A. M. Brun, A. Harriman, V. Heitz, J.-P. Sauvage, *J. Am. Chem. Soc.* **1991**, *113*, 8657–8663.
- [39] T. S. Balaban, M. Linke-Schaetzel, A. D. Bhise, N. Vanthuyne, C. Roussel, C. E. Anson, G. Buth, A. Eichhöfer, K. Foster, G. Garab, H. Gliemann, R. Goddard, T. Javorfi, A. K. Powell, H. Rösner, T. Schimmel, *Chem. Eur. J.* **2005**, *11*, 2267–2275.
- [40] G. M. Sheldrick, SHELXTL 5.1, Bruker AXS Inc., 6300 Enterprise Lane, Madison, WI 53719–1173, USA, **1997**.

Received: May 30, 2005  
Published online: November 28, 2005